Sciencexpress Research Article

Voyager Measurements of Hydrogen Lyman-α Diffuse Emission from the Milky Way

Rosine Lallement,[1,2]* Eric Quémerais,[2] Jean-Loup Bertaux,[2] Bill R. Sandel,[3] Vlad Izmodenov[4]

[1]GEPI, Observatoire de Paris, CNRS, Université Paris Diderot, Place Jules Janssen, 92190, Meudon, France. [2]LATMOS-IPSL, Université Versailles-St Quentin, Guyancourt, France. [3]Lunar and Planetary Laboratory, University of Arizona, Tucson, AZ 85719, USA. [4]Lomonosov Moscow State University, Moscow, Russia.

*To whom correspondence should be addressed. E-mail: rosine.lallement@obspm.fr

Doppler-shifted hydrogen Lyman-alpha (Lyα) emission from galaxies is currently measured and used in cosmology as an indicator of star formation. Until now, the Milky Way emission has not been detected, owing to far brighter local sources, including the H Glow, i.e., solar Lyα radiation backscattered by interstellar atoms that flow within the solar system. Because observations from the Voyager spacecraft, now leaving the heliosphere, are decreasingly affected by the H glow, the Ultraviolet Spectrographs are detecting Lyα diffuse emission from our galaxy. The surface brightness toward nearby star-forming regions is about 3 to 4 Rayleigh. The escape fraction of the radiation from the brightest H II regions is on the order of 3% and is highly spatially variable. These results will help constraining models of Lyα radiation transfer in distant galaxies.

The hydrogen Lyα emission line at 121.6 nm is ubiquitous in astrophysical objects. Diffuse emission in galaxies is generated through recombination cascades of interstellar hydrogen atoms following their ionization by UV photons from early-type stars in the so-called H II regions, or by collisions in interstellar shocks due to stellar winds and supernovae. During de-excitation Lyα arises from transitions from the $n = 2$ state to the ground state ($n = 1$), while Hα emission at 656.3 nm arises from transitions from the $n = 3$ to the $n = 2$ level. Theory indicates that 1.61 Lyα photons are produced for each Hα photon (*1*). Two important research fields in astrophysics imply the hydrogen Lyα emission. For cosmological redshifts between 0.3 and 6 Lyα is shifted to the near-UV and visible and used as a tracer of star-forming galaxies. A second major goal is the use of the 21 cm emission of neutral hydrogen, the transition between the hyperfine levels of the ground state, as a probe of the epoch of reionization, the formation of the first stars following the dark age of the Universe. In very low density or/and very cold media, absorption and subsequent reemission of Lyα photons influences the population distribution over the hyperfine levels (defining the spin temperature), linking in a complex way the 21 cm emission to the ambient Lyα radiation field, the Wouthuysen-Field effect (*2*, *3*). The interpretation of the 21 cm measurements must take the Lyα radiation field into account.

Because Hα is emitted along with Lyα in ionized regions, a strong link between the two types of radiation is in principle expected. However, the fate of Lyα photons is completely different and much more complex as compared to Hα. Typical H II regions consist of ionized gas surrounded by neutral envelopes (H I clouds). Because almost all interstellar H atoms are in their ground state, they do not absorb Hα photons; indeed the Hα radiation is a direct visible tracer of H II regions. By contrast, interstellar H I clouds are extremely opaque to Lyα. Inside these clouds, Lyα photons are absorbed and scattered many times, and their propagation is a random walk from their creation point through the interstellar H medium. Lyα photons produced in the ionized cores are thus trapped in the surrounding neutral gas. In evolved galaxies, their probability of absorption by a dust grain is subsequently much higher than for Hα, for a given distance in a straight line. One way for a Lyα photon to survive is to acquire a wavelength shift from line center, through multiple scattering in the H medium, because this allows longer distances of propagation. According to the most detailed models, almost all photons that escape H I clouds have been shifted from the cloud rest wavelength and the line shape consists of one or two peaks shifted from the rest frame by typically 2-4 Å (*4*). Refined models of the radiation transfer show that the intensity and line profile of the Lyα emerging from a galaxy depend on geometric properties, velocity fields of both ionized and neutral gas, dust and H_2 spatial distribution (*4*–*8*). Indeed, a strong variability of the intrinsic fluxes and line profile shapes has been observed among distant galaxies, with a poor correlation between the flux and other tracers of the star formation rate (*9*–*14*).

These sophisticated radiation transfer models have not been validated in situations for which gas density, dust content, geometry and kinematics are well known, such as the Milky Way H II regions. The reason is that, paradoxically, Lyα emission from our own galaxy has not been detected yet. Very close to late-type stars, diffuse Lyα emission may be generated through direct resonant scattering of the stellar Lyα line radiation by surrounding H atoms. This is the case around the Sun, both in planetary gaseous envelopes such as Earth's geocorona, and within the entire heliosphere due to interstellar H atoms that approach the Sun, causing the so-called H glow (*15*, *16*) (Fig. 1). These local sources are negligible compared to the galactic background, except for an observer located within the solar system where they become dominant. Contrary to external galaxies observations that benefit from enough wavelength shift between the emitter and the local matter, for our Galaxy there is no shift to prevent the contamination by the solar system.

Estimates of galactic Lyα brightness based on the UV photon production rate and the gas distribution range from tens to hundreds of Rayleigh (R) (*17*–*20*). By comparison, the geocoronal surface brightness varies between 1,000 and 20,000 R as viewed from rocket or satellite altitudes. From deep space it is not a contaminant, but the heliospheric H glow, whose brightness is of the order of 400-1,400 R for an observer at 1 AU, remains an obstacle for all observations within the inner heliosphere, not only because of its intensity but also its time and directional fluctuations in response to variations in the solar wind and solar radiation. This explains why it has been impossible to detect the weaker Galactic contribution. The expected pattern of the Galactic emission when observing from the Sun is also uncertain, which further complicates discrimination. Decreasing upper limits of 250, 50 then 40 R (*16*, *21*–*23*) were deduced from OGO-5, Mars-7 and Voyager data respectively, under the assumption of a nearly isotropic galactic emission. A firm upper limit of 15 R along 5 great circles was obtained using hydrogen absorption cell measurements (*24*). Attempts to detect the galactic signal by means of its spectral characteristics have not been conclusive. High resolution spectra recorded with HST (*25*) have not revealed any particular Doppler-shifted feature superimposed on the H glow line that would be the signature of propagation through very large optical paths.

We describe observations of the sky diffuse UV emission performed with the Ultraviolet Spectrograph (UVS) on board the two Voyager spacecraft since 1993. Our analysis aims at disentangling the Lyα emission of our heliosphere from distant emission of the Milky Way, and at measuring the brightness and properties of the latter emission.

Voyager UVS data analysis. The UVS instruments aboard Voyager 1 (V1) and Voyager 2 (V2) have been observing the Lyα diffuse emission since the beginning of the spacecraft cruise to the outer planets (*26*). The two spacecraft are now reaching the boundary of the heliosphere and they have moved away from the bright regions that are close to the Sun. As viewed from the Voyagers, the brightness of the Lyα diffuse emission has become as low as 40 R in the anti-solar direction, which is also close to the so-called upwind direction (where the interstellar wind comes from), located at about 20° from the galactic center (*22*, *23*, *27*). In addition, the local emission has become angularly smoother because solar wind influences on the H distribution decrease with distance. Finally, the solar emission variability at daily and monthly scales is now strongly attenuated by the opacity of intervening neutrals between the Sun and the outer heliosphere. These three effects work together to facilitate detecting a weak galactic contribution.

After 1993 special UVS measurements were performed using the scan platform on both spacecraft. A scan consists of long duration (several hours to one day) observations in 18 to 20 directions separated by about 10°, which permits observing the large scale intensity pattern over an entire hemisphere (Fig. 2). A scan pattern reflects the heliospheric structure, with a maximum brightness near the Sun, where the line-of-sight intercepts the most emissive region, and a minimum close to the anti-solar direction. Consecutive scans are slightly shifted in direction (Fig. 2), making it possible to probe degree- and even sub degree-scale variations (*22*, *28*). For V1, there are three types of scans, named A, B and C, that correspond to different swaths across the sky. For V2, there is only one type (Fig. 2). Scans are spread between 1993 and mid-2003 for V1, and between 1993 and mid-1998 for V2. These observations were initially motivated by the study of the so-called Hydrogen Wall, a region of enhanced H density due to a pile-up of interstellar matter and magnetic field in front of the heliosphere (Fig. 1), whose characteristics are diagnostics of the interaction between the solar wind and the circumsolar interstellar medium (*29*–*32*). That the region of the galactic center, a potential source of Lyα, lies by coincidence near the head of the heliosphere and the H wall brightness maximum has for a long time been a source of ambiguities in the data interpretation (*33*).

In most spectra only the Lyα line is detected (type 1 spectra, Fig. 2), and its intensity can be derived in a rather straightforward way by summing counts in the Lyα channels. But at low galactic latitudes the line is superimposed on a spectrally extended signal due to diffuse, dust scattered light of hot stars (Fig. 2, bottom). This emission traces the presence along the line-of-sight of interstellar dust within the H II regions where the UV light of young hot stars is ionizing the neutral hydrogen, and where subsequent recombinations of protons and electrons produce both Hα and Lyα. This UV light is thus closely associated with the Lyα sources. Using a Hα full-sky composite map (*34*), we clearly see that, for all scans, the directions having the brightest diffuse light clearly coincide with the Galactic Plane and bright Hα regions, which is expected (Fig. 2). The main H II regions crossed by the V1 A-B and V2 scans correspond to the Scorpius-Ophiuchus constellations. In this area the main contributors to the Hα emission are OB associations at distances of the order of 150 parsecs; other H II regions that are as far as 3,500 parsecs are also seen.

When those stellar continua are present, the inferred Lyα line intensity depends on their exact shape in the Lyα spectral region. In particular, we know that there must be a depression in the scattered starlight spectrum centered exactly at the same location as the emission line. This absorption trough is the combination of the intrinsic Lyα line in the spectrum of the illuminating star, augmented by the absorption by interstellar hydrogen atoms along the photon trajectories from the star to the scattering dust grain and finally to the observer (*35*, *36*). This trough must be taken into account in the computation of the Lyα line intensity (Fig. 2), but it can not be precisely measured with UVS because of its limited spectral resolution; it must be estimated. For the brightest H II regions the starlight is so intense that potential errors associated with simplified estimates are no longer negligible as compared to the small Galactic signal, thus we devised a method to disentangle the Lyα emission and the starlight continuum (SOM) based on the fact that for any stellar spectral type the absorption trough must appear very smooth, due to the instrumental response to an extended source. We have performed several simulations to test this method, and have checked it in two independent ways (SOM). We have also eliminated data showing a starlight continuum higher than a given threshold (*37*) and tested the influence of its level (SOM). In the course of the analysis of the spectra, we have also devised a method to correct for the background created in the detector by energetic particles emitted by the radioisotope thermoelectric generator (RTG, the Voyager energy source). This method is fully independent of the scattered light described above. Contrary to expectations, this background increased with time after about 1990 for both spacecraft, and began to fluctuate for V1 after 1999. Based on this temporal behavior we suspect that the UVS detectors are sensitive to heliospheric energetic particles in addition to the RTG particles. In our interpretation the flux of those particles increased during the approach of the solar wind termination shock for both spacecraft, and fluctuated during the multiple crossings of the shock by V1.

Scan measurements, model and Hα comparisons. We have treated the four types of scan separately, normalized them to correct for solar flux variations, averaged them together and accumulated the data in 19 or 20 angular bins. In doing so, we lost the sub-degree scale variability but gained in sensitivity. Uncertainties on the averaged intensity result from three main sources: (i) the energetic particle background subtraction, (ii) the small solar illumination fluctuations during a scan, (iii) the influence of the dust-scattered light subtraction. The uncertainty linked to the photon noise is negligible in comparison with those sources. The first two sources produce quasi-random fluctuations that can be estimated in different ways (SOM) and amount to less than 1% within a scan angular bin. The third source has a more complex behavior, with some potential systematic underestimate or overestimate depending on the level and shape of the continuum. According to our simulations, the error may reach 5% for an individual spectrum in the areas that have the highest level of dust-scattered light compatible with our threshold. This is why we display two error bars on the scan data: the first one $\sigma/\sqrt{n}$ is deduced from the data point dispersion σ within each bin, and represents the combination of three sources, assuming the third effect is totally random. The second one corresponds to the very conservative assumption that the third source is totally systematic (i.e. all brightness values are over- or under-estimated in a given bin) and thus does not decrease along with the averaging process within the bin. We have indications that such an error bar is actually more representative of the sub-degree scale brightness variability than a continuum removal effect (SOM).

We compared the data to a radiative transfer model of Lyα photons throughout the whole heliosphere. The model (*38*) was applied to time-dependent neutral hydrogen distributions computed in response to the solar wind and solar radiation during the last two solar cycles. The H atom distributions are based on a self-consistent model of the interaction between the variable sun and the interstellar flow. Charged particles were treated as a fluid, while neutral atoms were treated by a Monte-Carlo simulation. Intensities were calculated for the locations of the Voyagers and each line-of-sight. Model values computed for each data point were normalized and binned in exactly the same way as the data. In parallel, we use the Hα map to compute for each data point the Hα intensity that would be recorded for the same viewing conditions as for the Voyager scans.

Figures 3 and 4 display the data, the heliospheric model, and the Hα brightness. Overall, there is a very good agreement between the model and the data. Note the similarity between the model and the data for V1-A at scan angle 100 deg where one scan point deviates significantly from the mean trace on the sky to avoid a bright star. For the V1 scans, the model minima fall outside the galactic plane (where Hα is strong). For V1 A and B, these minima are located as in the data, but there is an excess in the data with respect to the model close to the Plane and a link between Hα bright regions and those enhancements. It is also clear that the Lyα enhancements start farther from the Plane than the Hα. Some changes in the intensity slope are also clearly found within regions that have no starlight, precluding any bias linked to this signal. At variance with A and B, the V1C scans cross the Plane in a very weak Hα area, and, as in response to this low level, they do not show clearly a marked excess close to Plane (Fig. 4). However they are not entirely smooth, and in particular one region outside the Plane (scan angle ≅ 170°) shows some enhancements. This angular structure along the scans is found for all individual scans (SOM) and thus can not be attributed to residual solar variations or particle background fluctuations. Moreover, the total absence of stellar continuum in this region precludes any particular problem associated with the starlight.

At variance with V1, for V2 the minimum in the heliospheric model falls near the Plane and the bright Hα area. The shapes of the model and the data are somewhat different, with the observed minimum shifted outside the Plane to larger scan angles. We interpret this shift as due to the presence of a galactic enhancement that modifies the location of the minimum. This confirms the correlation between galactic Lyα and Hα found for V1A and B scans. Outside the Plane, the model does not fit the data as well as for V1, which may be due to a galactic contribution extending outside the Plane, or to a potential small inadequacy of the model that appears for the V2 location. Allowing for a flatter model minimum, we have also drawn a smooth curve fitting as closely as possible the data below and above the Galactic plane, while keeping the modeled minimum location. Assuming that there is no galactic emission outside the Plane, the difference between this curve and the data at the Plane location provides an estimate of the weakest galactic excess in this area that is compatible with the data. In favor of the first solution and the validity of the model, we note that the excess measured for V2, in the region where V1A-B and V2 scans overlap (Fig. 2), is in good agreement with the excess determined for V1 (Figs. 3 and 4). This suggests, in the same way as for the V1C scans, that there may be Lyα enhancements outside the bright H II regions and up to 50° from the Plane.

We have derived from Figs. 3 and 4 the difference between the data and the model and converted it using the calibration factors of 70 R per count s^{-1} and 80 R per count.s^{-1} for V1 and V2 respectively (*23*, *39*). We derive an average value for the galactic brightness of about 3-4 R in the Scorpius-Ophiuchus area (Fig. 5). For Voyager 2 we show both the minimum and maximum values discussed above. Despite the large dispersion, there is a clear positive correlation between the two signals. As noted above, some Lyα enhancements have no Hα counterpart, and in general the amplitude of the Lyα variations is much smaller than for Hα, as shown by comparing the data with the fitted linear relationship between Lyα and Log(Hα).

Results and perspectives. Our analysis shows that, in addition to the smooth heliospheric emission, the UVS detects a galactic Lyα emission of the order of a few Rayleigh that is mainly concentrated on the plane of the Galaxy. The emission is weak enough to be compatible with existing upper limits. This result provides an estimate for the Lyα escape rate from the Milky Way for an outside observer. Enhancements are also detected outside the Galactic Plane, potentially explained by the presence of nearby H I clouds outside the Plane that scatter the Lyα radiation formed in H II regions within the Plane.

Of wide use for distant galaxies is the escape fraction, defined as the ratio of escaping to locally produced Lyα photons. For high redshift galaxies it is found to be a few percent (*14*). Fig. 5 shows that as seen from the Sun the escape fraction from the brightest H II regions is of the order of 3%, if we assume the classical Lyα/Hα production ratio of 1.61 and neglect the Hα absorption between the source region and the Sun. This percentage however increases strongly where Hα becomes weaker. When integrating over large fractions of the sky such areas become substantial contributors to the global escape fraction, in the same way the HI halo of nearby galaxies is found from recent observations to contribute to the Lyα emission (*41*).

Observations of distant galaxies also refer to the equivalent width $W_{Ly\alpha}$, which measures the fraction of light in the form of Lyα photons w.r.t. the adjacent UV continuum (*40*). $W_{Ly\alpha}$ is positive when Lyα is seen in emission and negative when it is seen in absorption. Usually it is integrated over a whole galaxy. However, recent spatially resolved observations (*41*) show that $W_{Ly\alpha}$ is globally increasing from negative values for central parts to highly positive values from surrounding haloes. Here we detect the variability of $W_{Ly\alpha}$ at a much smaller scale. Negative values of the order of 20-40 Å are found in the directions that correspond to bright starlight UV continua. They are negative because, after subtraction of the heliospheric line, the galactic emission line is not large enough to compensate for the stellar-interstellar absorption trough in the UV continuum. Where the continuum becomes smaller $W_{Ly\alpha}$ becomes positive (the line is seen in emission) and increases rapidly. By definition it cannot be defined (or is infinite) where the continuum becomes zero.

In the case of our Galaxy a huge amount of information is available on stars, gas and dust. Milky Way Lyα data can be used to test the complex radiative transfer models that are developed for distant galaxies or studies of the coupling between HI 21 cm and Lyα radiation fields in very low density media (*42*, *43*).

References and Notes

1. M. Brocklehurst, *Month. Not. Roy. Acad. Sci.* **153**, 471 (1971).
2. S. A. Wouthuysen, *Astron. J.* **57**, 31 (1952).
3. G. B. Field, *Astrophys. J.* **129**, 551 (1959).

4. D. A. Neufeld, *Astrophys. J.* **350**, 216 (1990).
5. S. Charlot, S. M. Fall, *Astrophys. J.* **415**, 580 (1993).
6. S. Richling, *Astrophys. Space Sci.* **284**, 361 (2003).
7. M. Hansen, S. P. Oh, *Month. Not. Roy. Acad. Sci.* **367**, 979 (2006).
8. A. Verhamme *et al.*, *Astron. Astrophys.* **460**, 397 (2006).
9. J. Lequeux *et al.*, *Astron. Astrophys.* **301**, 18 (1995).
10. C. Gronwall *et al.*, *Astrophys. J.* **667**, 79 (2007).
11. J.-M. Deharveng *et al.*, *Astrophys. J.* **680**, 1072 (2008).
12. G. Östlin *et al.*, *Astron. J.* **138**, 923 (2009).
13. K. A. Kornei *et al.*, *Astrophys. J.* **711**, 693 (2010).
14. M. Hayes *et al.*, *Nature* **464**, 562 (2010).
15. J. L. Bertaux, J. E. Blamont, *Astron. Astrophys.* **11**, 200 (1971).
16. G. E. Thomas, R. F. Krassa, *Astron. Astrophys.* **11**, 218 (1971).
17. 1 Rayleigh (R) = $10^6/4\pi$ photons $\mathrm{cm}^{-2}\ \mathrm{s}^{-1}\ \mathrm{sr}^{-1}$.
18. G. E. Thomas, J. E. Blamont, *Astron. Astrophys.* **51**, 283 (1976).
19. B. T. Draine, E. E. Salpeter, *Nature* **271**, 730 (1978).
20. W. D. Vacca *et al.*, *Astrophys. J.* **460**, 914 (1996).
21. J. L. Bertaux *et al.*, *Astron. Astrophys.* **46**, 19 (1976).
22. E. Quémerais *et al.*, *Astron. Astrophys.* **308**, 279 (1996).
23. E. Quémerais *et al.*, *J. Geophys. Res.* **108**, 8029 (2003).
24. R. Lallement *et al.*, *Astron. Astrophys.* **140**, 243 (1984).
25. J. T. Clarke *et al.*, *Astrophys. J.* **499**, 482 (1998).
26. A. L. Broadfoot *et al.*, *Space Sci. Rev.* **21**, 183 (1977).
27. E. Quémerais *et al.*, *Astrophys. J.* **711**, 1257 (2010).
28. The field-of-view is a 0.1° x 0.87° rectangle. The signal was integrated over the 9 UVS spectral channels that define the Lyα emission. Lines-of-sight close to nearby hot stars were avoided. The photon Poisson noise is always smaller than 2% due to the long exposure time. For a given heliospheric hydrogen distribution, the local glow brightness is proportional to the total solar output, which varies with time. The mean brightness level of the H glow is thus slowly varying with the solar cycle phase. Small variations may also exist within a scan due to anisotropic illumination coupled to solar rotation, but they are limited by the multiple scattering effects and should not exceed a few percent. Further details on the instrument and the data are given in (*22*) and in SOM.
29. V. B. Baranov, Y. G. Malama, *J. Geophys. Res.* **98**, 15157 (1993).
30. V. V. Izmodenov *et al.*, *J. Geophys. Res.* **104**, 4731 (1999).
31. N. V. Pogorelov *et al.*, *Astrophys. J.* **696**, 1478 (2009).
32. J. L. Linsky, B. E. Wood, *Astrophys. J.* **463**, 254 (1996).
33. E. Quémerais *et al.*, *Astron. Astrophys.* **299**, 249 (1995).
34. D. P. Finkbeiner, *Astrophys. J.* **146**, 407 (2003).
35. B. Savage, R. Panek, *Astrophys. J.* **191**, 659 (1974).
36. R. H. Buss *et al.*, *Astrophys. J. Lett.* **454**, L55 (1995).
37. The stellar continuum count level must be lower than approximately 10% of the central Lyα channel count level.
38. E. Quémerais *et al.*, *Astron. Astrophys.* **488**, 351 (2008).
39. Cross-calibrations have been performed with a number of other instruments. Our conservative estimated error on the calibration factor is 30%.
40. The equivalent width of an emission line is defined as the wavelength interval over which the continuum around the line must be integrated to produce the same intensity as the observed line. It corresponds to the surface of the line when the spectrum is normalized in such a way the continuum level is 1 and has no dimension. Note that in Fig. 2 the line contains both heliospheric and galactic contributions, thus it can not be used to obtain a visual representation of the galactic line equivalent width.
41. C. C. Steidel *et al.*, 2011, arXiv:1101.2204
42. H. Liszt, *Astron. Astrophys.* **371**, 698 (2001).
43. S. Baek *et al.*, *Astron. Astrophys.* **495**, 389 (2009).

Acknowledgments: We thank J. Holberg for kindly providing Voyager spectra of early-type stars.

Supporting Online Material

www.sciencemag.org/cgi/content/full/science.1197340/DC1
SOM Text
Figs. S1 to S11
References

3 September 2010; accepted 16 November 2011
Published online 1 December 2011; 10.1126/science.1197340

Fig. 1. Simplified scheme of the Lyα diffuse emission sources: (left) photons of solar origin are scattered by interstellar hydrogen atoms flowing within the solar wind (yellow area) and by interstellar atoms from the H wall around the heliosphere where the interstellar gas is piling-up (green area). Galactic photons originate within the Milky Way ionized gas (right). The direction of the Sun's motion within the local interstellar cloud, i.e. of the front of the heliosphere, by chance, nearly coincides with the galactic center. Consequently the H wall maximum brightness, seen from inside the heliosphere, corresponds to an intense region of the Milky Way, illustrated here (right side) by the corresponding fraction of the Hα sky

Fig. 2. Scan data point directions superimposed on the Hα map from (*34*), in ecliptic coordinates. Four series of scans cross the Galactic Plane. Dashed arrows correspond to increasing scan angles. Solar and anti-solar directions as seen from V1 and V2 are shown by yellow and black diamonds. Data points marked by black arrows and labeled "type 1" have spectra such as those shown at bottom left. For "type 2" spectra recorded close to the Plane, dust-scattered starlight is superimposed (bottom right). The total Lyα emission is the

sum of the emerging line (black hatched area) and of the absorption line known to exist in the starlight continuum (red hatched area). The color scale for the scan data points (grouped in clusters) indicates the intensity of the continuum, with red indicating its absence and blue the most intense. The oval encircles the high latitude V1-C enhancement.

Fig. 3. Average normalized total Lyα surface brightness along the V1 A and B scans (black markers and axis), along with the corresponding heliospheric model (red markers and axis), the slit average Hα brightness (green squares and axis), the galactic latitude and zero latitude line (in violet). The green horizontal line is the average Hα surface brightness outside the Galactic Plane. The model scaling was chosen so that data and model agree in the last portion of the scan. Shown in red is the error bar deduced from the data point dispersion within a bin. In black is the very conservative uncertainty computed assuming a fully systematic error in starlight removal. The normalized intensity value of 1 corresponds roughly to 40 Rayleigh.

Fig. 4. Same as Fig. 3 for V1-C and V2 scans. V1-C scans show deviations from a smooth curve, especially at 170°. For V2, the model (red markers and right red axis) is adjusted to the data at scan angle 220°. The data is not compatible with the model minimum position. We also show an *ad hoc* smooth profile (pink curve) that satisfies the position of the minimum but has a slightly different shape.

Fig. 5. Difference between the data and the model, derived from Figs. 3 and 4 and attributed to the galactic emission, as a function of Hα. Error bars are the most conservative ones (drawn in black in Figs. 3 and 4). Circles are for the V1 scans (black, red and blue resp. for A, B, and C scans). Triangles are for V2, for the two cases in Fig 4. Shown are the adjusted linear relationships between Lyα and Log(Hα) for V1 (dashed black line) and all data points (red line).

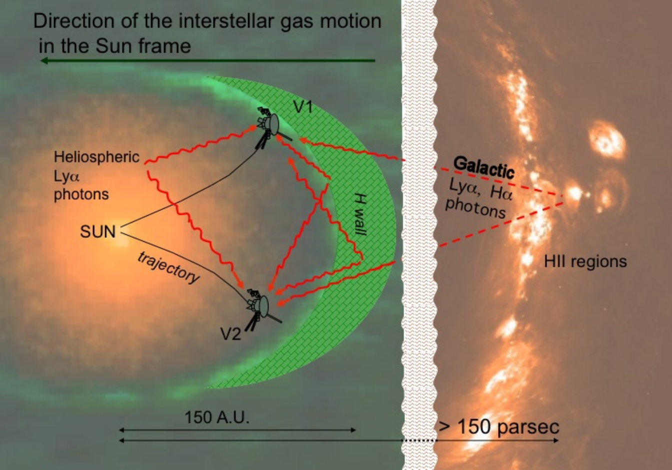
Direction of the interstellar gas motion in the Sun frame
V1
Heliospheric Lyα photons
SUN
trajectory
H wall
V2
Galactic
Lyα, Hα photons
HII regions
150 A.U.
> 150 parsec

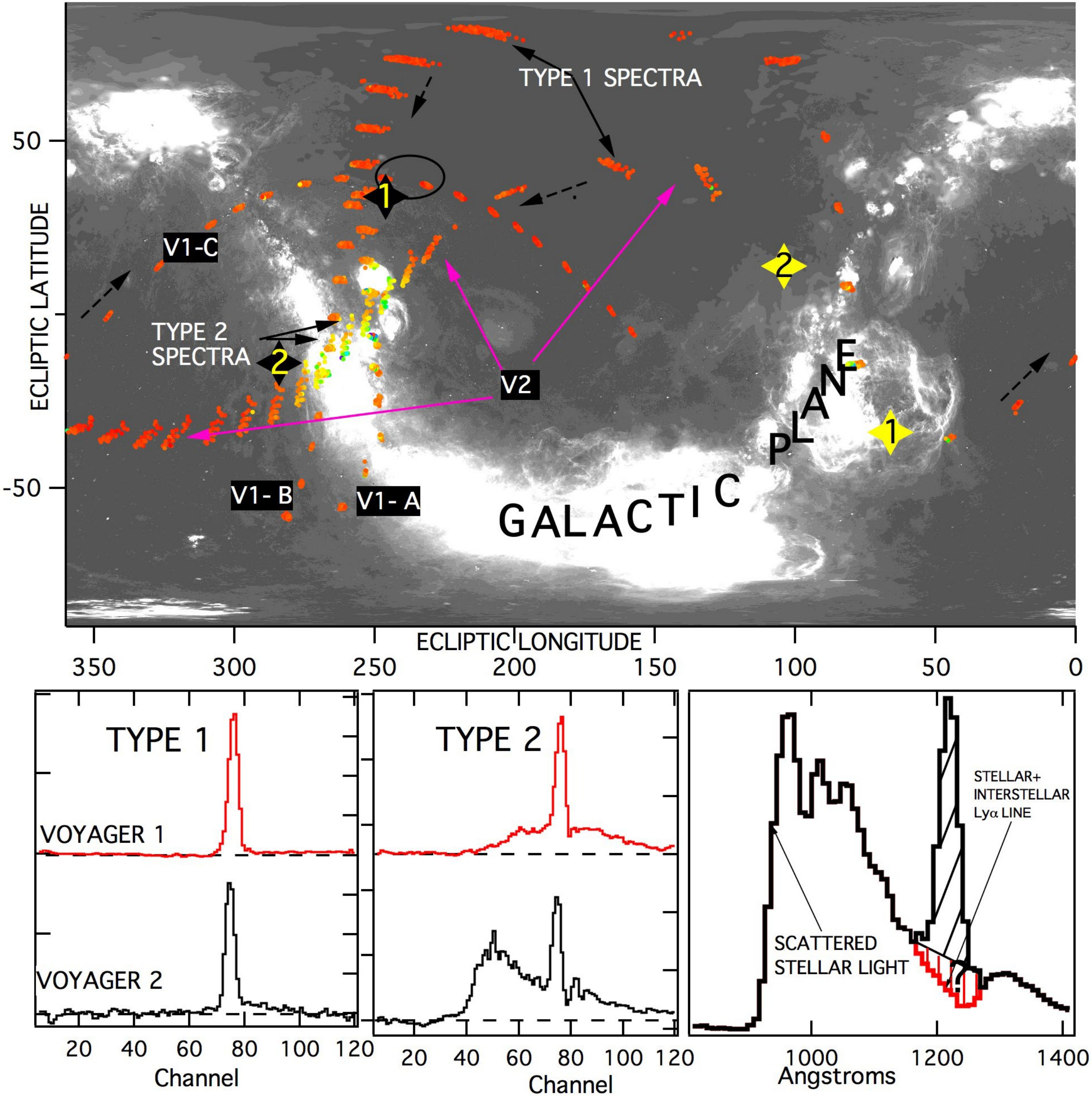
TYPE 1 SPECTRA
TYPE 2 SPECTRA
1
2
V1-C
V1- B
V1- A
V2
GALACTIC PLANE
ECLIPTIC LATITUDE
50
-50
ECLIPTIC LONGITUDE
350
300
250
200
150
100
50
0
TYPE 1
VOYAGER 1
VOYAGER 2
20
40
60
80
100
120
Channel
TYPE 2
Channel
SCATTERED STELLAR LIGHT
STELLAR+ INTERSTELLAR Lyα LINE
?
1000
1200
1400
Angstroms

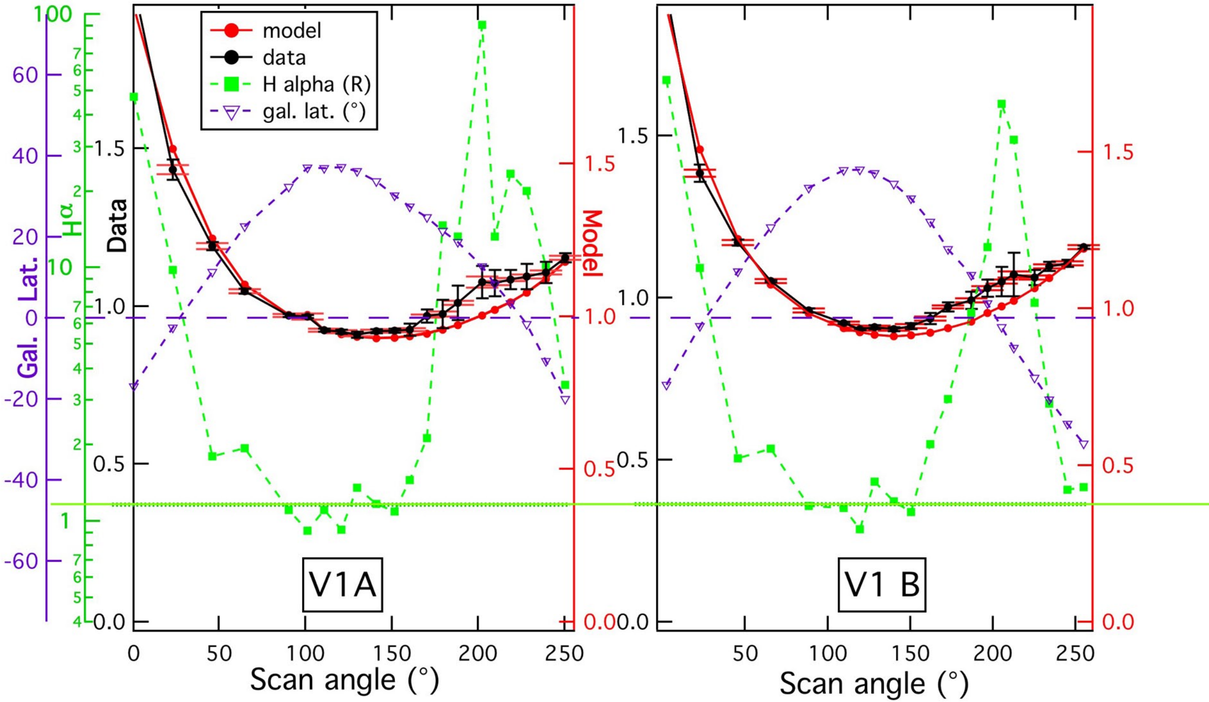

model
data
H alpha (R)
gal. lat. (°)
Gal. Lat.
Hα
Data
Model
60
40
20
0
-20
-40
-60
100
10
1
1.5
1.0
0.5
0.0
V1A
V1 B
0
50
100
150
200
250
Scan angle (°)

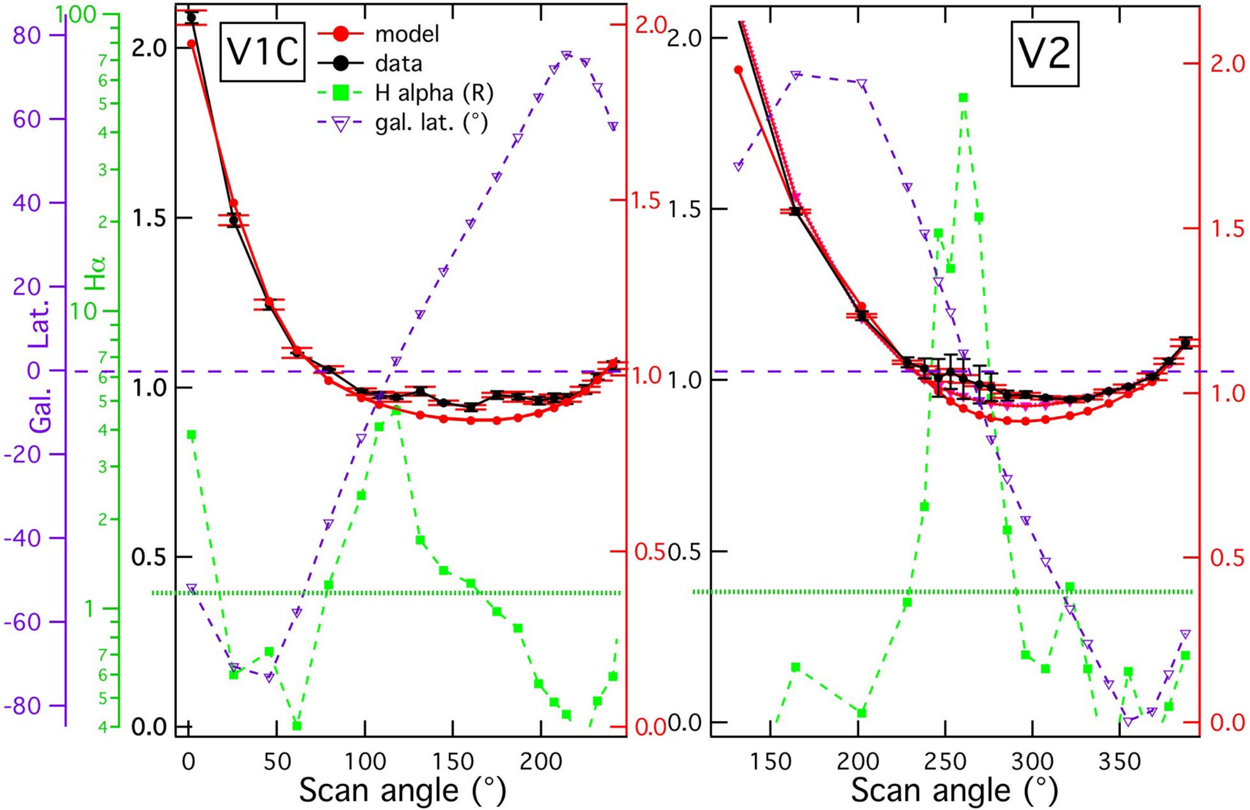
V1C
V2
model
data
H alpha (R)
gal. lat. (°)
Gal. Lat.
Hα
80
60
40
20
0
-20
-40
-60
-80
100
10
1
2.0
1.5
1.0
0.5
0.0
Scan angle (°)
0
50
100
150
200
250
300
350

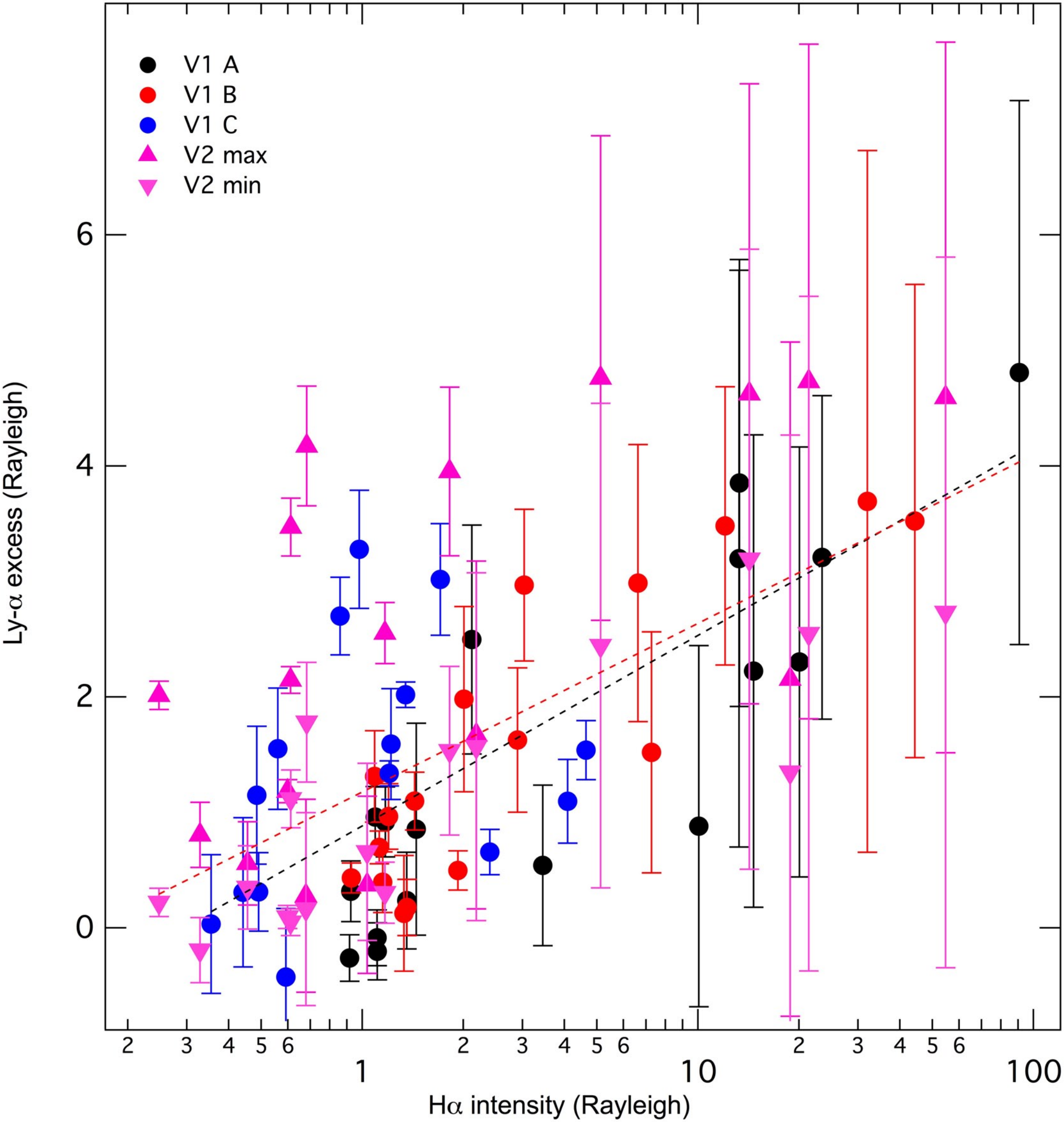
V1 A
V1 B
V1 C
V2 max
V2 min
Ly-α excess (Rayleigh)
Hα intensity (Rayleigh)
0
2
4
6
2
3
4
5
6
1
2
3
4
5
6
10
2
3
4
5
6
100